

Chaotic Advection in a Three-dimensional Volume Preserving Potential Flow

L. D. Smith^{1,2}, D. R. Lester¹ and G. Metcalfe³

¹CSIRO Mathematics Informatics and Statistics
 Graham Rd, Highett, Victoria 3190, Australia

²Department of Mechanical Engineering
 Monash University, Clayton, Victoria 3800, Australia

³CSIRO Materials Science and Engineering
 Graham Rd, Highett, Victoria 3190, Australia

Abstract

Scalar transport in a time-periodic 3D incompressible potential flow is studied in the context of Lagrangian chaos in a reoriented 3D dipole flow. A mixture of chaotic dynamics and regular KAM-tubes are observed, and particles reside on adiabatic surfaces rather than invariant surfaces. The factors controlling the adiabatic surfaces are investigated, for instance the presence of hyperbolic periodic points acts as a local accelerant to dynamics, yet also forms a barrier to transport. The adiabatic surfaces provide a mechanism for 3D scalar transport and the possibility of global chaos.

Introduction

Transport of a passive scalar is one of the most fundamental processes within a fluid flow. It is quantified by the advection equation

$$\dot{\mathbf{x}} = \mathbf{v}(\mathbf{x}, t), \quad (1)$$

with $\nabla \cdot \mathbf{v} = 0$ for incompressible flow; here \mathbf{v} is the fluid velocity field, t is time, and \mathbf{x} is physical space. The domain Ω of \mathbf{x} is the state space of the dynamical system. The study of (1) from a dynamical systems perspective has generated significant and novel insights into transport and mixing [8]. In terms of mixing a key consideration is whether a passive scalar visits every point within the flow domain. Since (1) is a non-linear dynamical system it can exhibit chaotic dynamics when there are at least three degrees of freedom. These dynamics are independent of the flow dynamics, hence chaos is possible even in slow, smooth (non-turbulent) flow.

Significant progress has been made in two-dimensional (2D) incompressible flows due to the formal analogy with Hamiltonian systems, for which the theoretical framework, tools and techniques can be directly applied. The tools of Hamiltonian mechanics have led to various insights into transport in e.g. geophysical flows, microfluidics, and industrial mixing.

Conversely, much less is known about three-dimensional (3D) flows [10]. A reason for this is that the Hamiltonian analogy breaks down at stagnation points of 3D systems. These points play an important role in the generation of chaotic dynamics in 3D systems [1]. The 3D generalisation of the Kolmogorov–Arnold–Moser (KAM) Theorem [3] is not as strong as the 2D version, which plays a key role in analysing the Lagrangian topology of 2D systems. Furthermore, the 3D state space allows for richer topological structures and more complex dynamics. Currently the theory behind 3D systems is less well-developed [10], highlighting the need for fundamental research into 3D systems. The gap in understanding is being bridged by recent works, for e.g. [1, 2, 7, 9], of which a main focus is 3D chaos, which is a rich field at the forefront of research.

While 3D inviscid flows and Stokes flows have received atten-

tion, few studies have considered potential flows, which have widespread applications within e.g. porous media, groundwater and packed column flows. Steady potential flows are irrotational, thus homoclinic/heteroclinic connections between stable and unstable manifolds which are hallmarks of chaos cannot form, meaning potential flows can stretch but not fold fluid elements. This is unique to potential and Darcy flows, those in which the helicity $\boldsymbol{\omega} \cdot \mathbf{v}$ is identically zero, whilst other steady 3D flows (inviscid, Stokes) can admit chaos. To produce chaotic particle trajectories it is therefore required to invoke transient flows, which allow crossing of streamlines.

One of the simplest transient 3D flow protocols involves rotation of a dipole about an equator. The equatorial rotation protocol is closely related to the corresponding 2D analogue [6], which found that for certain parameter choices chaotic advection and global transport are possible. Since the 3D system can be viewed as an extrusion of the 2D system, one expects that for certain parameter choices particles will advect chaotically in two dimensions, however, it isn't clear what transverse dynamics (perpendicular to the surface) should be expected. There are three possibilities: the particles could be confined to invariant surfaces with no transverse dynamics and hence no 3D transport; the particles could reside on adiabatic surfaces with slow transverse dynamics; or transverse dynamics could be fast, yielding a truly 3D flow.

Steady three-dimensional flow

To construct a time-dependent 3D flow, we consider a steady base flow generated by a 3D dipole, with source/sink at $(0, 0, \pm 1)$. We introduce time-periodic reorientations of this flow to create an unsteady flow. This flow is axisymmetric about the z -axis, therefore cylindrical coordinates (ρ, θ, z) form a natural system to describe it. The simplest reorientation is a rotation of the dipole about an axis perpendicular to z . Unlike the 2D dipole flow [6], the unbounded 3D flow does not possess a rotationally symmetric separating stream surface at $r = 1$. We therefore confine the dipole flow to reside within the unit sphere Ω . The flow potential Φ is governed by

$$\nabla^2 \Phi = 0, \text{ and } \mathbf{n} \cdot \nabla \Phi|_{\partial\Omega} = 0, \quad (2)$$

where \mathbf{n} is the outward normal to the boundary $\partial\Omega$. To solve these equations we use the method of images [4] for the Neumann boundary problem (2), yielding an analytic solution for Φ , the contours of which are shown in Figure 1a. Due to axisymmetry, \mathbf{v} may be described by the Stoke's stream function Ψ where $\mathbf{v} = \nabla \times (\Psi/\rho)\hat{\mathbf{e}}_\theta$,

$$\Psi(\rho, z) = \frac{1 - z^2 - \rho^2}{4\pi} \left(\frac{1}{\sqrt{(1-z)^2 + \rho^2}} + \frac{1}{\sqrt{(1+z)^2 + \rho^2}} \right).$$

Fluid streamlines reside on stream-surfaces of constant Ψ . Along with the azimuthal angle θ , this is a pair of invariants of

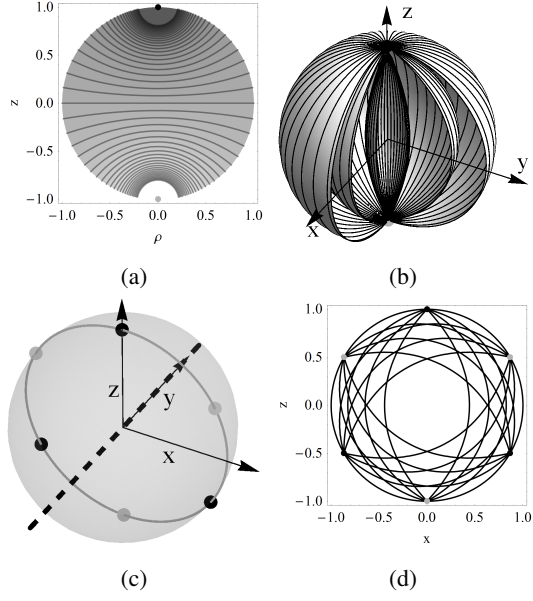


Figure 1: (a) Contours of the axisymmetric potential function Φ . (b) Level surfaces of the axisymmetric stream function Ψ . (c) Reorientation protocol for $\Theta = 2\pi/3$. (d) Superposed stream function contours under rotation $\Theta = 2\pi/3$.

the steady flow \mathbf{v} , i.e. $\nabla G \cdot \mathbf{v} = 0$ for $G = \Psi, \theta$. The streamlines of \mathbf{v} are given by the orthogonal intersections of level surfaces of Ψ with level surfaces of θ , shown in Figure 1b.

We denote by $\tilde{\Upsilon}_t$ the dynamical systems flow of \mathbf{v} , satisfying

$$\tilde{\Upsilon}_0(\mathbf{X}) = \mathbf{X}, \text{ and } \frac{d}{dt} \tilde{\Upsilon}_t(\mathbf{X}) = \mathbf{v}(\tilde{\Upsilon}_t(\mathbf{X})),$$

where \mathbf{X} denotes Lagrangian coordinates. Symmetries of the flow $\tilde{\Upsilon}_t$ govern the Lagrangian topology of the system and impose constraints upon scalar transport. The base flow possesses two basic symmetries: axisymmetry about the z -axis and a reflection reversal symmetry in the xy -plane. Algebraically these can be written as

$$\tilde{\Upsilon}_t = R_\gamma^z \tilde{\Upsilon}_t R_{-\gamma}^z, \quad (3)$$

$$\tilde{\Upsilon}_t = S_{xy} \tilde{\Upsilon}_t^{-1} S_{xy}^{-1} \quad (4)$$

respectively, where R_γ^z is rotation by γ about the z -axis and S_{xy} is reflection in the xy -plane. We discuss the affect reorientation has on these symmetries later.

Transient three-dimensional flow

We consider the simplest class of reorientation protocol, consisting of an equatorial rotation. The dipole is rotated by some fixed angle Θ (Figure 1c), and remains at each position for some fixed non-dimensional time τ (scaled such that $\tau = 1$ is the emptying time of Ω). This flow is called the 3D RPM flow, the transient velocity field of which can be approximated as

$$\tilde{\mathbf{v}}(\mathbf{x}, t) = \mathbf{v}(R_{\lfloor x \rfloor \Theta}^y \mathbf{x}, t) \quad (5)$$

where R_λ^y is rotation by λ about the y -axis, and $\lfloor x \rfloor$ denotes the integer part of x . If the viscous time scale $1/\kappa$ is small, where κ is the fluid kinematic viscosity, then transient effects associated with dipole reorientations as quantified by the Strouhal number $St = Re/\tau$ may be ignored. Since we assume the Reynolds number is negligible, the piecewise steady velocity approximation (5) is exact (except in the limit $\tau \rightarrow 0$).

If Θ is incommensurate with π , then the dipole positions are dense on the equator, whilst if $\Theta = (n/m)2\pi$ then the dipole positions are periodic with period m . Without loss of generality we only consider the case where the equator lies in the xz -plane, with rotation of the dipole about the y -axis.

While the steady flow has two invariants, θ and Ψ , neither are preserved under rotation. This breakdown is necessary for global transport for otherwise particles would remain on invariant surfaces, making 3D transport impossible. This notion is discussed in more detail later.

Particle tracking

To form a closed flow domain to study transport, we impose periodic boundary conditions at the dipole, such that a particle exits the sink and is instantaneously re-injected at the source with the same values of Ψ and θ .

To visualise long-time dynamics of the 3D RPM flow we use a Poincaré map which captures the particle position after each period τ , defined by

$$\Upsilon = R_\Theta^y \tilde{\Upsilon}_\tau.$$

Note that the map Υ tracks particles in the Lagrangian dipole frame, but since the Lagrangian topology is invariant under the rotation R_Θ^y the dynamics of the map Υ are equivalent to the continuous map in the laboratory frame.

We refer to the Poincaré map of a particle as the set of images of the particle over a large number of iterations of the map Υ . Figure 2 shows a typical Poincaré map, with regular (non-chaotic) regions topologically distinct to ergodic (chaotic) regions.

It is not possible to find an analytical form for the flow $\tilde{\Upsilon}_t$, numerical particle tracking via direct integration of the advection equation (1) is required. Since the dynamical system is conservative, $\nabla \cdot \mathbf{v} = 0$, it follows that both the flow $\tilde{\Upsilon}_t$ and the map Υ are volume preserving. Therefore in order to preserve the topological structure of the conservative dynamical system it is important to use an explicitly volume preserving numerical method. For 2D Hamiltonian systems there exist a wide class of symplectic methods which explicitly conserve the Hamiltonian, which in the context of chaotic advection corresponds to area preservation. For 3D systems such techniques do not apply as Hamiltonian systems are even-dimensional. We therefore adapt the method in [5] in which the 3D system is broken down via operator splitting of the advection equation into three 2D systems on which symplectic integration can be used. This enables us to produce volume preserving integrators of arbitrary order; we use a fourth order Gauss–Legendre method.

Symmetries of the map Υ

Symmetries play an important role in organising fluid transport, as they can constrain dynamics and Lagrangian topology. The symmetries (3) and (4) of the base flow $\tilde{\Upsilon}_t$ transform to yield two symmetries of Υ . First, as a special case of the axisymmetry property (3), the base flow is symmetric in the xz -plane, i.e. $\tilde{\Upsilon}_t = S_{xz} \tilde{\Upsilon}_t S_{xz}^{-1}$. As a result Υ satisfies

$$\Upsilon = R_\Theta^y \tilde{\Upsilon}_\tau = R_\Theta^y S_{xz} \tilde{\Upsilon}_\tau S_{xz}^{-1} = S_{xz} R_\Theta^y \tilde{\Upsilon}_\tau S_{xz}^{-1} = S_{xz} \Upsilon S_{xz}^{-1}$$

and is therefore also symmetric in the xz -plane. As the xz -plane is an invariant surface of Υ , the dynamics in the y^+ and y^- hemispheres mirror each other and so without loss of generality we only consider transport in the y^+ hemisphere. The xz -plane thus acts as an impenetrable barrier, dividing Ω in two.

The other symmetry of Υ is obtained via the reflection reversal symmetry (4) as follows,

$$\Upsilon = R_\Theta^y \tilde{\Upsilon}_\tau = R_\Theta^y S_{xy} \tilde{\Upsilon}_\tau S_{xy}^{-1} = R_\Theta^y S_{xy} \Upsilon^{-1} R_\Theta^y S_{xy}^{-1} = S_1 \Upsilon^{-1} S_1 \quad (6)$$

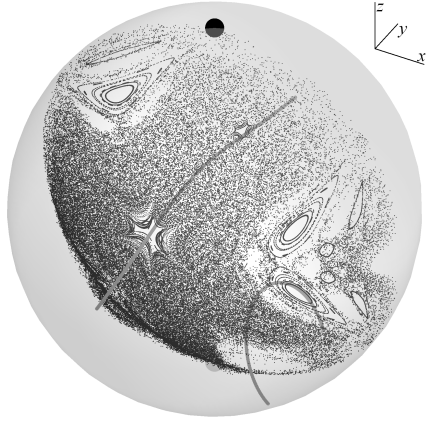


Figure 2: The Poincaré maps of a collection of particles for $(\Theta, \tau) = (2\pi/3, 0.1)$. The period one lines are shown in grey.

where $S_1 = R_{\Theta}^y S_{xy}$. One can compute that S_1 is the map that reflects a point through the plane $z = \frac{-\sin\Theta}{\cos\Theta+1}x$. Therefore structures in the Lagrangian topology must evolve symmetrically about this plane also, illustrated in Figure 2 and Figure 3b by the reflectional symmetry of the coherent structures.

Periodic lines

Periodic points and lines form the basis of Lagrangian topology in that they give explicit conditions for both local chaos and local non-mixing regions. The stability of the local Lagrangian dynamics of periodic points forms the global dynamics of the system, and creates a template upon which transport plays out.

A point \mathbf{X} is said to be periodic if $Y^n(\mathbf{X}) = \mathbf{X}$ for some n . The minimum such n is called the order of \mathbf{X} . In 2D it is only possible for isolated periodic points to occur, however in 3D it is possible to have more complex structures, such as periodic lines. The lower order points play a greater role in affecting the dynamics so these are the main focus.

In order to find the period one points of the 3D RPM flow, we exploit the symmetry (6) which guarantees that all period one points must lie on the plane of symmetry $z = \frac{-\sin\Theta}{\cos\Theta+1}x$. One can then easily find all the period one points on the line intersecting the xz -plane. The local stability of the points can be computed by calculating the eigenvalues λ_i of the linearised deformation tensor $DY(\mathbf{X}) = (\partial Y^i / \partial X^j)|_{\mathbf{X}}$ which quantifies the rate of stretching near \mathbf{X} over one iteration of Y . Since $\nabla \cdot \mathbf{v} = 0$, it follows that $\prod \lambda_i = 1$. If $|\lambda_i| = 1$ for all eigenvalues, then there is a local rotation but no stretching, and the point is called elliptic. If $|\lambda_i| > 1$ for some eigenvalue, then a fluid particle is stretched in the direction of the corresponding eigenvector, and contracted in the direction of the eigenvector(s) corresponding to $|\lambda_j| < 1$. Such points are called hyperbolic and are linearly unstable. In the case that one of the eigenvalues is equal to one, it is known that the point lies on a period one line, and the line continues in the direction of the corresponding eigenvector. This gives us a means to search for all period one lines, and also determine their stability, illustrated by Figure 2 and Figure 4.

Attached to hyperbolic points are two invariant structures, the stable and unstable manifolds. The unstable manifold is the collection of points whose backward trajectories converge to the given point, and the stable manifold is the set of points whose forward trajectories converge to the given point [8]. Intersections between stable and unstable manifolds form homoclinic/heteroclinic connections, and are a hallmark of chaotic dynamics. Hyperbolic points are thus synonymous with chaos.

Results and Discussion

If the spherical domain Ω were foliated by topologically distinct invariant surfaces of the map Y , then each particle would be confined to an invariant surface, and 3D transport would not be possible, even though dynamics within an invariant surface may be chaotic. Figure 2 and Figure 3b show that the trajectories of the map Y resemble ‘shells’ which could form invariant surfaces. However, Figure 3c shows that an associated ‘shell number’ G varies slowly in time, meaning particles belong to a so-called ‘adiabatic surface’, which is not strictly invariant, but transport is slow. This is important because it provides a mechanism for local 3D transport and chaos.

Adiabatic surfaces

A natural way to explain why these adiabatic surfaces occur is to consider the invariant G of the base flow \tilde{Y}_t defined as follows. While Ψ, θ are one invariant pair of the flow, there exist an infinite number of pairs, and so we may construct another invariant from Ψ, θ . First consider the streamline given by $\Psi = \psi_0$ and $\theta = \pi/2$, call it T (see Figure 3a). If we rotate this streamline by $\pi/2$ about the y -axis to form T' , the surface formed by the union of all streamlines that pass through T' is a level surface S_{ψ_0} of G . The surfaces S_{ψ_0} foliate the entire hemisphere, and are mutually disjoint. For a general point (x, y, z) in the hemisphere $G(x, y, z)$ is defined to be the unique value ψ_0 such that (x, y, z) lies on the surface S_{ψ_0} . Explicitly

$$G(\rho, \theta, z) = \Psi(\tilde{\rho}(\Psi(\rho, z)) \sin \theta, \tilde{\rho}(\Psi(\rho, z)) \cos \theta),$$

where $\tilde{\rho}(\psi) = \sqrt{1 + 2\pi^2\psi^2 - 2\pi\sqrt{2\psi^2 + \pi^2\psi^4}}$ is the unique value of ρ such that $\Psi(\rho, 0) = \psi$. Thus by construction G is an invariant of the base flow \tilde{Y}_t . For the transient 3D RPM flow, G is close to being invariant under rotation about the y -axis, so the map Y produces small perturbations in G , as seen in Figure 3c.

We exploit the disparity in the time-scales of the dynamics—while intra-surface dynamics can be fast, the advection transverse to G is slow—by introducing canonical action-angle variables. There exists a theoretical framework for action-angle variables [7], and they can be used to classify the flow dynamics. Action variables vary slowly with time, whereas angle variables vary rapidly, so for example an action-action-angle system can be thought of as one-dimensional. The fact that G experiences minor perturbations from the map Y means that we can use it as an action variable, while two other variables are needed to describe the intra-surface dynamics.

Within the sphere there exist regular tubular regions which act as a barrier to particle transport, particles can neither leave nor enter. The tubes result from elliptic segments of periodic lines, whereby particles oscillate around the periodic point, and form either closed paths (the ‘loops’ in Figure 2) or chaotic regions between loops (similar to KAM-tori). Due to the essentially 1D nature of the closed loops, these tubular regions can be described using action-action-angle coordinates.

Conversely, there are regions topologically distinct from the tubes (the ergodic region in Figure 2 and Figure 3b), within these regions one still has the action variable G , but particles travel ergodically around the adiabatic surface. These regions therefore require action-angle-angle coordinates. Unlike the tubes, these regions allow fully 3D transport within them, and thus provide a mechanism for 3D transport.

It should be noted that when particles from the ergodic regions come into close proximity to the elliptic regions one of the angle coordinates slows considerably and one could consider these regions to also be called action-action-angle. This can be seen by

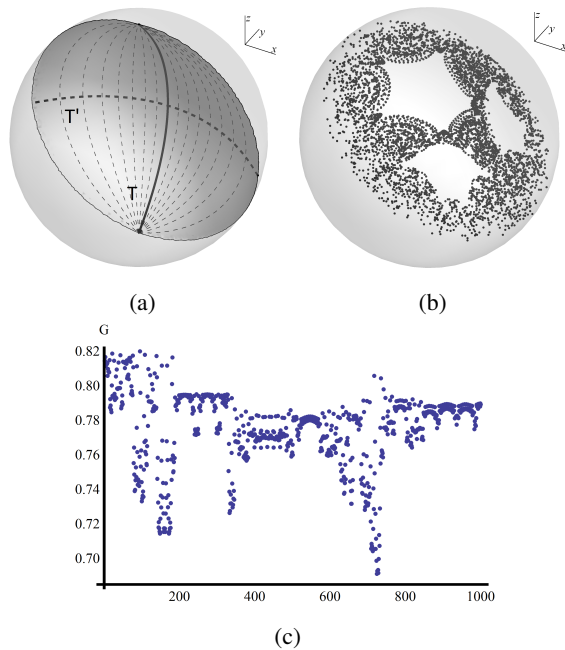


Figure 3: (a) A level surface of G . The thick solid line is T , the thick dashed line is T' , and the dashed lines are streamlines of \tilde{Y}_t that pass through T' . (b) Poincaré map of a particle with $(\Theta, \tau) = (2\pi/5, 0.1)$. (c) Perturbations of the invariant G as the particle is advected for 1000 iterations. The scaling is such that $G = 1$ and $G = 0$ correspond to the xz -plane and the spherical boundary respectively.

the punctuated regions of Figure 3c in which the shell-jumping becomes small and quasi-periodic. The point oscillates around the ‘islands’ (seen in Figure 3b) for long periods of time until a ‘crisis’ occurs and the point jumps to a new island.

Confinement due to invariant manifolds

Advection transverse to adiabatic surfaces plays a central role in governing transport in the 3D RPM flow. Therefore understanding the controlling mechanics of transverse advection is the key to understanding global transport and the application of transport theories for canonical variables. Figure 4 indicates that the stable and unstable manifolds of the period-one points play an important role. These manifolds associated to hyperbolic points near the parabolic point form a ‘leaky’ barrier, with fast transport inside and slow transport outside. The faster rate of transverse transport within the barrier can be attributed to the hetero-

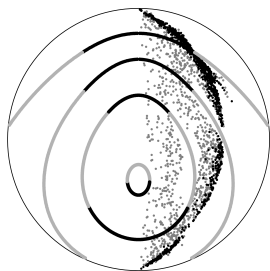


Figure 4: Cross-section through the symmetry plane $z = \frac{-\sin\Theta}{\cos\Theta+1}x$, showing the period one lines (black: hyperbolic, grey: elliptic); the Poincaré maps of three points that lie in the same ergodic region (grey points); and the unstable manifold of a hyperbolic point near the parabolic point (black points). For the protocol $(\Theta, \tau) = (2\pi/3, 1.1)$.

clinic/homoclinic connections that exist within the region, causing rapid stretching and folding of fluid parcels. Combined with the impenetrable KAM-tubes, such features build up a complete picture of global transport in the 3D RPM flow.

The nature of the ‘leaky’ surface provides a focus for future study, it is still unclear whether particles can leak across the surface, and if it is a surface of locally minimal flux. Since global chaos within each hemisphere will only be possible if all periodic points are hyperbolic, future investigation should also focus on whether there exist choices of the protocol parameters Θ, τ which permit only hyperbolic points.

Conclusions

We have studied chaos in a 3D transient potential flow, specifically the 3D RPM flow. The use of a volume-preserving integration technique is employed to preserve the conservative nature of the dynamical system. The flow possesses two symmetries, one which divides the sphere into two non-mixing hemispheres, and another which imposes reflectional symmetry in the Lagrangian topology. We see a mixture of dynamics, with the existence of both chaotic regions and KAM-tubes which prevent mixing. Within the chaotic regions, adiabatic surfaces are observed, and provide a means for 3D transport, with transverse motion acting as a slow ‘action’ variable. We provide a geometric interpretation of these surfaces, and discuss the impact of the stability of periodic points. In particular, hyperbolic points allow fast transverse dynamics, yet their stable/unstable manifolds also act as a surface of minimal flux. These studies provide novel insights into chaotic transport in 3D potential flows, and provide a direction for future work.

References

- [1] Bajer, K., Hamiltonian Formulation of the Equations of Streamlines in three-dimensional Steady Flows, *Chaos Solitons & Fractals*, **4**, 1994, 895–911.
- [2] Cartwright, H.E., Feingold, M. and Piro, O., Chaotic advection in three-dimensional unsteady incompressible laminar flow, *J. Fluid. Mech.*, **316**, 1996, 259–284.
- [3] Cheng, C.-G. and Sun, Y.-S. Existence of invariant tori in three-dimensional measure preserving mappings, *Cel. Mech.*, **47**, 1990, 275–292.
- [4] Dassios, G. and Sten, J.C.-E, On the Neumann function and the method of images in spherical and ellipsoidal geometry, *Math. Meth. Appl. Sci.*, **35**, 2012, 482–496.
- [5] Finn, J.M. and Chacón, L., Volume preserving integrators for solenoidal fields on a grid, *Phys. Plasmas*, **12**, 2005, 054503.
- [6] Lester, D.R. *et al.*, Lagrangian topology of a periodically reoriented potential flow: Symmetry, optimization and mixing, *Phys. Rev. E*, **80**, 2009, 036208.
- [7] Mezić, I. and Wiggins, S., On the integrability and Perturbation of Three-Dimensional Fluid Flows with Symmetry, *J. Nonlinear Sci.*, **4**, 1994, 157–194.
- [8] Ottino, J.M., *The kinematics of mixing: stretching, chaos, and transport*, Cambridge University Press, 1989.
- [9] Speetjens, M.F.M., Clercx, H.J.H. and van Heijst, G.J.F., Merger of coherent structures in time-periodic viscous flows, *Chaos*, **16**, 2006, 043104.
- [10] Wiggins, S., Coherent structures and chaotic advection in three dimensions, *J. Fluid. Mech.*, **654**, 2010, 1–4.